Recovery of Molybdenum, Chromium, Tungsten, Copper, Silver, and Zinc from Industrial Waste Waters Using Zero-Valent Iron and Tailored Beneficiation Processes

Authors:

Daniel Vollprecht, Katharina Plessl, Simone Neuhold, Fritz Kittinger, Wolfgang Öfner, Peter Müller, Robert Mischitz, Klaus Philipp Sedlazeck

Abstract:

Zero-valent iron (ZVI) has been used for water treatment for more than 160 years. However, passivation of its surface often constituted a problem which could only be tackled recently by the innovative Ferrodecont process using a fluidized bed reactor. In this study, pilot scale experiments for the removal of Mo, Cr, W, Cu, Ag and Zn from two industrial waste water samples and lab-scale experiments for the beneficiation of the abrasion products are presented to integrate the Ferrodecont process into a complete recycling process chain. Firstly, 38.5 % of Cu was removed from sample A, yielding abrasion products containing 33.1 wt% Cu as metallic copper (Cu) and various Cu compounds. The treatment of sample B removed 99.8 % of Mo, yielding abrasion products containing 17.8 wt% of Mo as amorphous phases or adsorbed species. Thermal treatment (1300 °C) of the abrasion product A indicated a reduction of delafossite to metallic Cu according to differential scanning calorimetry (DSC), thermogravimetry (TG) and X-ray diffraction (XRD), which was successfully separated from the magnetic iron phases. Hydrometallurgical treatment (1.5 M NaOH, 3 d, liquid:solid ratio (L:S) = 15:1) of sample B yielded aqueous extracts with Mo concentrations of 5820 to 6300 mgL?1. In conclusion, this corresponds to an up to 53-fold enrichment of Mo during the entire process chain.

Article

Recovery of Molybdenum, Chromium, Tungsten, Copper, Silver, and Zinc from Industrial Waste Waters Using Zero-Valent Iron and Tailored Beneficiation Processes

Daniel Vollprecht [1],*[ID], Katharina Plessl [1], Simone Neuhold [1][ID], Fritz Kittinger [1], Wolfgang Öfner [1], Peter Müller [2], Robert Mischitz [2] and Klaus Philipp Sedlazeck [1]

[1]   Montanuniversität Leoben, Franz-Josef-Straße 18, 8700 Leoben, Austria;
      katharina.plessl@stud.unileoben.ac.at (K.P.); simone.neuhold@unileoben.ac.at (S.N.);
      fritz.kittinger@unileoben.ac.at (F.K.); wolfgang.oefner@unileoben.ac.at (W.Ö.);
      philippsed@gmail.com (K.P.S.)
[2]   ferroDECONT GmbH, Peter-Tunner-Str. 19, 8700 Leoben, Austria; peter.mueller@ferrodecont.at (P.M.);
      robert.mischitz@ferrodecont.at (R.M.)
*   Correspondence: daniel.vollprecht@unileoben.ac.at

Abstract: Zero-valent iron (ZVI) has been used for water treatment for more than 160 years. However, passivation of its surface often constituted a problem which could only be tackled recently by the innovative Ferrodecont process using a fluidized bed reactor. In this study, pilot scale experiments for the removal of Mo, Cr, W, Cu, Ag and Zn from two industrial waste water samples and lab-scale experiments for the beneficiation of the abrasion products are presented to integrate the Ferrodecont process into a complete recycling process chain. Firstly, 38.5 % of Cu was removed from sample A, yielding abrasion products containing 33.1 wt% Cu as metallic copper (Cu) and various Cu compounds. The treatment of sample B removed 99.8 % of Mo, yielding abrasion products containing 17.8 wt% of Mo as amorphous phases or adsorbed species. Thermal treatment (1300 °C) of the abrasion product A indicated a reduction of delafossite to metallic Cu according to differential scanning calorimetry (DSC), thermogravimetry (TG) and X-ray diffraction (XRD), which was successfully separated from the magnetic iron phases. Hydrometallurgical treatment (1.5 M NaOH, 3 d, liquid:solid ratio (L:S) = 15:1) of sample B yielded aqueous extracts with Mo concentrations of 5820 to 6300 mgL^{-1}. In conclusion, this corresponds to an up to 53-fold enrichment of Mo during the entire process chain.

Keywords: critical metal removal; industrial waste water; Ferrodecont process; zero-valent iron; hydrometallurgy; thermal treatment

1. Introduction

Tungsten (W) and molybdenum (Mo) are considered critical raw materials, defined as metals with growing economic importance that might be susceptible to future scarcity, by the European Union [1]. Like other critical metals, Cr and W occur in industrial waste waters [2]. However, critical metals are mostly not recovered in standard chemical-physical waste water treatment as they often have no negative impact on the environment. Contrary, for chromium (Cr), copper (Cu), silver (Ag), and zinc (Zn) maximum allowed limits for indirect and direct discharge of waste water exist in Austria [3]. Consequently, several methods for their removal like precipitation by neutralization and reduction exist and are industrially applied [4]. However, the valorisation of the removed metals, i.e., the further treatment of the resulting abrasion products for separation of iron from non-ferrous metals, is not considered, but very important for closing the loop.

Recently, a new approach to remove these metals from synthetic aqueous solutions and original industrial waste water samples using zero-valent iron (ZVI) in a fluidized bed reactor (FBR) has been developed. This "Ferrodecont process" was developed between 2009 and 2011 for the remediation of Cr(VI)-contaminated sites [5] and is based on a reaction between solid ZVI granules and dissolved metal species which are removed from the solution due to reduction and/or adsorption and/or precipitation processes.

The complex nature of the underlying chemical reactions of ZVI in aqueous solutions has been discussed intensely yielding "a review of reviews" [6] which is beyond the scope of this study. In summary, ZVI is either considered as reducing agent or as adsorbing and reducing agent. The corrosion of ZVI to Fe^{2+} and the reaction of the latter with H_2O_2 may yield the strongly oxidizing hydroxyl radical OH• [7]. Reduction is relevant for metals like Cr [5] which have various oxidation states, whereas adsorption on or incorporation into iron corrosion products takes also place in other cases. A detailed literature review regarding the interaction of critical metals with ZVI is found in our previous study [2]. For example, adsorption of Cu [8] as well as of Mo and W [9] onto ferrihydrite, removal of Mo by maghemite nanoparticles [10], incorporation of W into ferromangenese oxides [11] and the removal of Zn [12] and Ag [13] and its incorporation into ferrites [14] have been described.

In our previous study [2] the feasibility of the process for the fixation of critical and potentially critical metals was demonstrated and a paradigm shift from disposal to recycling was initiated. Firstly, synthetic aqueous solutions and industrial waste waters were treated with ZVI in a batch reactor (overhead shaker), and secondly industrial waste waters were treated in a fluidized bed reactor. The resulting abrasion products were analysed for chemical and mineralogical composition and it was found that more than 90% of Cr, V and nickel (Ni) were removed from the solution and mainly adsorbed to lepidocrocite (γ-FeOOH), or present in specific mineral phases which were characteristic for a particular industrial waste water [2].

However, for an actual recycling the removed metals need to be separated from the iron phases. Consequently, the purpose of the present study is an integrated approach in which two industrial waste waters containing (A) Cu, Ag, and Zn, and (B) W, Cr, and Mo were treated in a pilot scale Ferrodecont process, abrasion products were separated from the solution by a centrifuge, dried, analysed for chemical and mineralogical composition and further treated by (A) alkaline leaching and (B) a combination of thermal treatment and magnetic separation. These last steps allow separation of Cu, Ag, Zn, W, Cr, and Mo from iron (Fe) and yield nonferrous metals concentrates for direct hydro- and pyrometallurgical recycling for samples A and B, respectively.

In summary, the significance of this study is that we integrate a fluidized bed reactor using ZVI into an entire process chain transforming industrial waste waters into high-purity secondary raw materials for metallurgy. The aim of this work is to demonstrate that metals cannot only be removed from industrial waste waters by the Ferrodecont process, but truly recycled by subsequent beneficiation processes. The conclusion is that our suggested process chains work for specific waste water samples, but tailored recipes are required for every single waste water.

2. Materials and Methods

2.1. Industrial Waste Water Characterization

Two industrial waste water samples (1000 L), A and B, were obtained from industrial partners. Sample A represents a waste water from copper metallurgy, whereas sample B represents a leachate from a ferrous slag landfill. After determination of the pH, subsamples were taken by a syringe, filtrated (d = 0.45 μm) and analysed for chemical composition using the screening mode based on ÖNORM EN ISO 17294-2 [15] by inductively coupled plasma mass spectrometry (ICP-MS, Agilent 7500 cx).

2.2. Ferrodecont Process

A pilot scale FBR was constructed at ferroDECONT GmbH, to conduct metal removal experiments using ZVI (Figure 1).
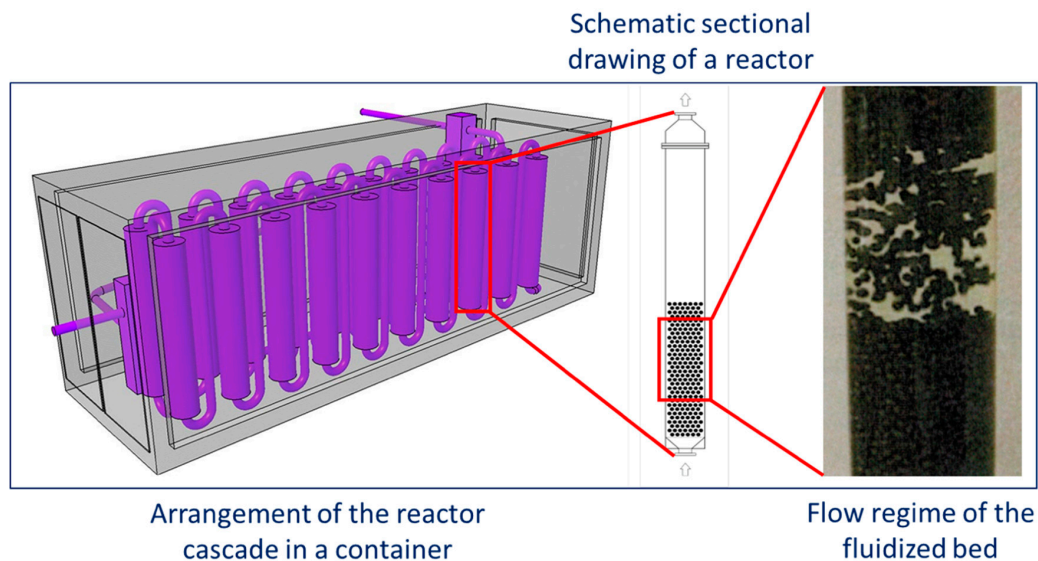

Figure 1. Scheme of the fluidized bed reactor (FBR).

Prior to the experiments the pH of sample B was adjusted to a value of 4 using HCl as the Ferrodecont process is known to work best at this pH [2] due to increased corrosion, whereas the pH of sample A was not modified (original value: 4.6). The industrial waste water was pumped with a flow of 1 Ls^{-1} into the reactor from the bottom to the top where it interacted with the ZVI granules (d = 4 to 6 mm, voestalpine Stahl Donawitz AG, austenite + cementite + magnetite + graphite + ledeburite, 4.3 wt% C). Each of the five reactors (height: 180 cm, inner diameter 70 cm) was filled to one third by ZVI with a bulk density of 4,640 kgm^{-3}. Due to the volume flow of the waste water a fluidized bed was created which filled about two third of the reactor. During the treatment, dissolved oxygen (O_2) concentration, electric conductivity, redox potential and pH were monitored. After discharge from the reactor, the water including the abrasion products was collected and pumped into the reactor again, creating a closed circuit. During the experiments compressed air (<0.1 bar above the system pressure) was injected into the reactor to increase iron corrosion. Intermediate samples of the solution were taken after 1, 2, and 3 h for sample A and after 3 and 25 h for sample B. After an experimental duration of 4 h (sample A) and 26 h (sample B, the longer experimental duration was chosen to ensure the complete reduction of Cr(VI)), suspensions were discharged from the reactor and abrasion products were separated from aqueous solution using a centrifuge (Gea Westfalia KG 2006, volume flow 600 Lh^{-1}, pressure 0.8 bar).

2.3. Characterization of Purified Aqueous Solutions and Obtained Abrasion Products

Purified aqueous solutions, obtained after centrifugation, were sampled with a spoon (V = 500 mL), filtrated (d = 0.45 μm) and analysed for chemical composition via ICP-MS as described for initial waste waters.

Abrasion products were dried at 105 °C until constant weight for material characterization and further experiments. Mineralogical analyses of abrasion products were conducted by X-ray diffraction (XRD, Pro PANalytical X'Pert Pro, operated with Co-Kα radiation at 40 mA, 45 kV and sample rotation; data were collected in a 2θ angle range between 4° and 110° and an increment of 0.02°). For chemical analyses, the abrasion products were digested in aqua regia according to ÖNORM EN 13657 [16]. Chemical analyses were conducted according to ÖNORM EN ISO 17294-2 [15] by using an ICP-MS system (Agilent 7500 cx).

2.4. Thermal Treatment and Magnetic Separation

For beneficiation of the abrasion products, two different approaches were chosen. For the abrasion product of sample A, a thermal treatment followed by magnetic separation was selected as reduction of Cu oxides to elemental Cu should occur according to the corresponding phase diagram [17] For the abrasion product of sample B, a hydrometallurgical treatment was chosen, as Mo is adsorbed to iron corrosion products as oxyanion [8] and should be desorbed at alkaline pH due to the repelling effect of identical charges, i.e., between the negatively charged MoO_4^{2-} anion and the negatively charged iron hydroxide surface.

Simultaneous thermal analyses (STA, Netzsch STA 449 C), a combination of differential scanning calorimetry (DSC) and thermogravimetry (TG), was conducted with a subsample (15 mg) of the dried abrasion product obtained from sample A. A heating rate of 10 °Cmin^{-1} was applied for the temperature range from 30 to 1350 °C. Nitrogen (N_2) was used as atmosphere.

Subsequently, a similar thermal treatment was conducted with another subsample of the dried abrasion product obtained from sample A. The sample was placed in an Al_2O_3 crucible which was put into a second graphite crucible. The crucible combination was placed in a vertical furnace (Gero Carbolite) which was rinsed with nitrogen and heated to 1300 °C at a rate of 6 °Cmin^{-1}. Afterwards, the temperature was kept constant for 1 h and the sample was removed from the furnace and cooled at room temperature.

The heated sample was further divided: One subsample was analysed for mineralogical composition by XRD as described for the untreated abrasion product. A second subsample was used to produce a polished section, on which electron microprobe analyses (EMPA, Superprobe JEOL JXA 8200) was performed to determine the elemental distribution of Fe, Cu, Ag, Ca, Si, P, S, O, and Cl using an accelerating voltage of 15 kV and a beam current of 10 nA. A third subsample was used for magnetic separation to remove the magnetic iron oxide fraction from the copper concentrate. The working distance between the magnet and the sample was set to 4 and 8 mm in two experiments to study the effect on yield and purity of the reject fraction, i.e., the copper product.

2.5. Hydrometallurgical Treatment

The abrasion product of sample B was subjected to two different hydrometallurgical leaching experiments in a beaker glass. Each 5 g sample was suspended in 75 mL 1.5 M NaOH and stirred for 3 d, but temperature was set to 50 and 70 °C in different experiments. After the experiments, solids were separated from aqueous solutions, using filtration (d = 2 μm). The liquids were filtrated additionally at 0.45 μm prior to chemical analyses by ICP-MS as described in Section 2.1. The resulting filter cakes were analysed for chemical composition after aqua regia digestion as described in Section 2.3.

3. Results and Discussion

3.1. Industrial Waste Water Characterization

Major cations in industrial waste water A (pH 4.6) are Ca (208 mgL^{-1}) and Mg (150 mgL^{-1}), but Cu (14.3 mgL^{-1}), Zn (9.93 mgL^{-1}) and Ag (1.26 mgL^{-1}) might be valuable metals for recovery (Table 1). Due to high Ca contents, it is suggested that waters from carbonate rocks, e.g., dolomite, were used in the copper plant. The high Cu and Zn content is in agreement with the role of these elements as main alloying element in brass. With respect to further recycling it has to be mentioned that both elements can be co-processed in copper plants [18] and also Ag is recovered there [19].

In comparison, in industrial waste water B (pH 10.4), Na (1333 mgL^{-1}) and K (500 mgL^{-1}) are the dominant cations and Mo (160 mgL^{-1}), W (20.7 mgL^{-1}), and Cr (45.7 mgL^{-1}) represent interesting metals for recovery. The high content of alkali metals might be due to a use of salts or bases in the plant, whereas Mo, W, and Cr are typical alloying elements in the steel industry.

Table 1. Chemical composition of industrial waste water samples.

Sample	Analyte (mgL^{-1})																	
	Na	Mg	Si	K	Ca	V	Cr	Mn	Fe	Ni	Cu	Zn	Se	Sr	Mo	Ag	W	pH
A	15.8	150	3.71	5.42	208	0.51	<0.02	4.61	4.46	1.93	14.3	9.93	<0.10	5.92	0.05	1.26	<0.01	4.6
B	1333	9.02	15.5	500	67.4	1.87	45.7	<0.02	<0.1	<0.02	0.08	<0.10	2.28	0.15	160	<0.01	20.7	10.4

3.2. Ferrodecont Process

During the treatment of sample A, the electric conductivity of the sample was at or above the upper limit of the measuring range of 13.4 mScm^{-1}. This can be explained by the high content of dissolved ions, including those which were not analysed, e.g., anions, organic species or NH_4^+. The dissolved O_2 concentration at the inlet of the reactor decreased from 5.5 mgL^{-1} to 0.8 mgL^{-1} after the waste water circulated several times through the reactor, which can be explained by oxygen consumption for ZVI oxidation. The dissolved O_2 concentration at the outlet of the reactor was significantly lower, but followed the same trend. Significant fluctuations of the measuring signal occurred which makes a quantitative statement difficult. Differences between inlet and outlet appeared because of corrosion processes, i.e., ZVI oxidation, during the reaction pathway. pH increased over reaction time at the inlet from 4.6 to 5.7, which can be explained by the consumption of protons for iron corrosion. Similarly, at the outlet, pH increased from 4.5 to 5.7. The redox potential at the inlet decreased from 540 to 130 mV which is in agreement with the observed decrease in dissolved O_2. At the outlet, the redox potential also shows a decreasing trend, but again shifted towards lower values, i.e., from 320 to 80 mV, which is in agreement with the other observations. With respect to the efficiency of the process, the decrease in dissolved O_2 concentration and redox potential and the increase in pH shift the system away from the optimum process conditions. Air injection might be an option to maintain the parameters in the ideal range.

Contrarily to the treatment of sample A, in case of sample B the electric conductivity of the sample increased from 11.2 mScm^{-1} to the upper limit of the measurement range (13.4 mScm^{-1}) at the inlet and was in a similar range at the outlet. This increase is due to the addition of HCl. Interestingly, the conductivity of sample B is initially smaller than that of sample A, although significantly higher cation concentrations were determined in sample B. It is suggested that other ions, e.g., organic compounds, contribute to the higher conductivity of sample A. The increase of the conductivity in sample B is very quick and occurs parallel to the adjustment of pH from 10.4 to 4.0. This suggests that acidification is related with the dissolution of suspended matter which might have been present in the sample. Additionally, the added chloride ions contribute to the increased conductivity. As with sample A, the dissolved O_2 concentration also decreased in sample B, but showing a maximum after 5 h because of air injection. In contrast to sample A, no differences between inlet and outlet dissolved O_2 concentrations were observed at distinct reaction times. This suggests a more homogeneous reaction regime throughout the entire reactor in terms of equally strong oxidation of ZVI at the inlet and outlet. After the initial pH adjustment to a value of 4, a steady increase to values of about 6 occurred, both at the inlet and the outlet of the reactor. This is in agreement with observations from sample A and can be explained by the same mechanisms. The redox potential decreased from 400 mV to less than 100 mV at the inlet and outlet which is also in accordance with sample A. With respect to process conditions, air injection temporarily increased O_2 concentrations which is positive to create adsorption sites for dissolved metals, but over a long term process parameters also shifted away from the ideal range.

3.3. Characterization of Purified Aqueous Solutions and Obtained Abrasion Products

For sample A, during the course of the experiment (4 h), the Cu concentration decreased from 14.3 mgL^{-1} to 8.88 mgL^{-1}, Zn concentrations from 9.93 mgL^{-1} to 7.96 mgL^{-1} and Ag concentrations from 1.26 mgL^{-1} to 0.75 mgL^{-1} (Figure 1). Furthermore, Ca concentrations (not shown) decreased from 208 mgL^{-1} to 190 mgL^{-1}. This suggests a removal from the solution and fixation in the obtained

abrasion products. In our previous study [2] we partly reached higher removal rates, but also observed tremendous differences between individual waste waters ranging from constant concentrations to removal rates above 90%. In summary, the moderate removal of metals in the present study is in agreement with previous results. Simultaneously, Fe concentrations increased from 4.46 mgL^{-1} to 5.54 mgL^{-1} which can be explained by partial dissolution of iron and incomplete re-precipitation as corrosion products.

The obtained abrasion product was separated in the wet state with a total weight of 553 g. According to ICP-MS analyses, the dried abrasion product is composed of 33.1 wt% Cu, 27.3 wt% Fe, and 3.92 wt% Ca (Figure 2). All other analysed elements are each below 1 wt%. The formation of a product, rich in Cu and Fe, is in qualitative agreement with the decrease of the dissolved concentrations of these elements. However, from a quantitative point of view, i.e., considering mass balances, liquid analyses combined with the sample volume yield a Cu loss of only 5 g, whereas solid analyses combined with solid weight suggests 183 g Cu to be present in the abrasion product. Even if the water content of the abrasion product is considered, it can be concluded that Cu was already present as suspended particulate matter in the industrial waste water prior to the experiment. Additionally, losses, e.g., during the filtration of the sample, have to be considered. Finally, not the total solid could be recovered by centrifugation which creates additional errors.
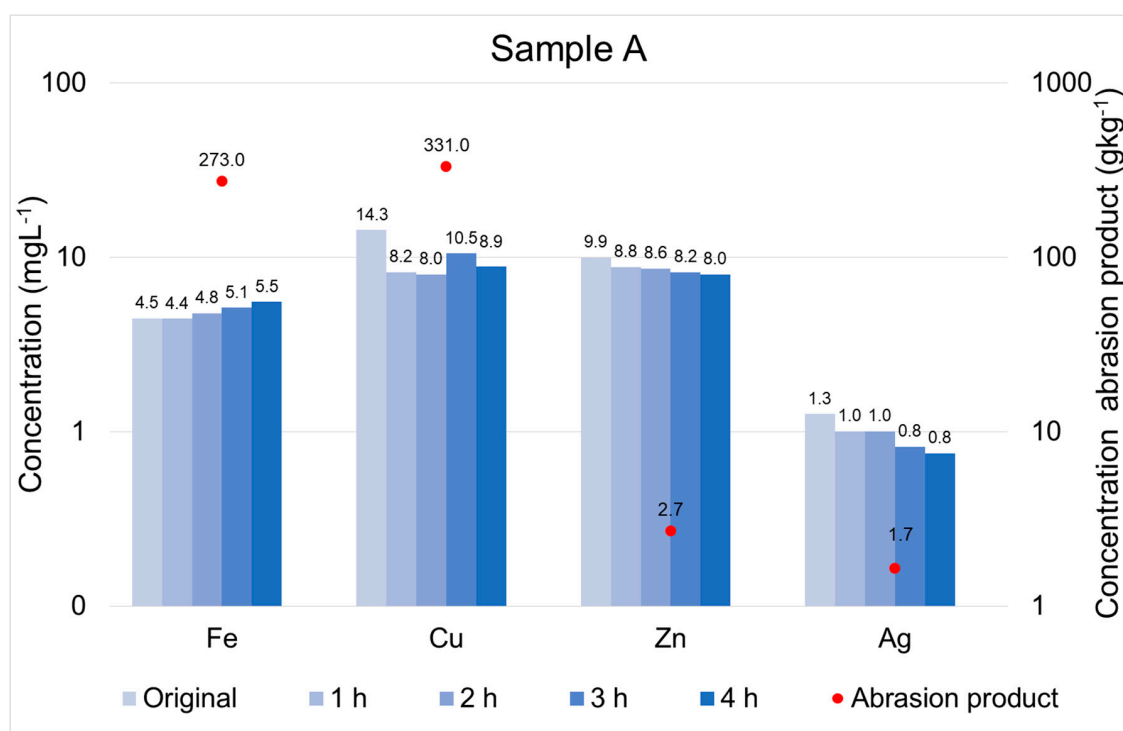

Figure 2. Evolution of the dissolved concentrations (blue bars) and concentrations in the resulting abrasion product (red dots) of Fe, Cu, Zn, and Ag during the Ferrodecont treatment of sample A.

XRD analyses (Figure 3) reveal that Cu is present as metallic Cu, delafossite (CuFeO$_2$), cuprite (Cu$_2$O), paratacamite (Cu$_2$(OH)$_3$Cl) and calcium copper oxide (CaCuO$_2$), whereas Fe is bound to goethite (α-FeOOH), lepidocrocite (γ-FeOOH) and also delafossite. With respect to recycling, the presence of metallic Cu is positive, whereas the presence of Cu compounds indicates further requirement for beneficiation. Regarding the iron phases, it can be concluded that complete oxidation to Fe(III) might have been supported by air injection, as in our previous study [2] also Fe(II)-containing magnetite (Fe$_3$O$_4$) was formed. Considering the mass balance, it is suggested that most of the Cu phases were already present as suspended particulate matter in the initial waste water. However, the drop in dissolved Cu concentration and the intense interaction between Cu species and ZVI suggests that a part of the delafossite might have formed during the Ferrodecont process.
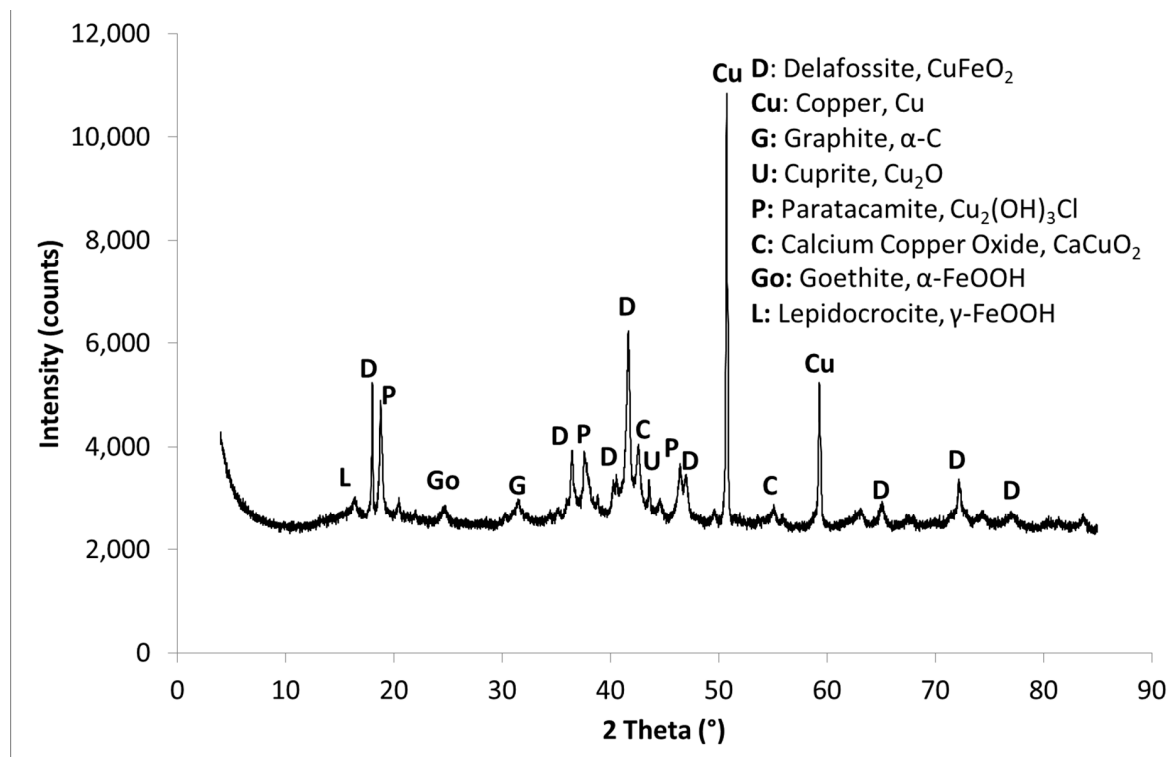
Figure 3. X-ray diffraction (XRD) pattern of the abrasion product obtained from Ferrodecont treatment of sample A.

For sample B, during the experimental duration (26 h), the dissolved Mo concentration decreased from 160 mgL^{-1} to 0.35 mgL^{-1}, that of Cr from 45.7 mgL^{-1} to 1.91 mgL^{-1} and that of W from 20.7 to 0.20 mgL^{-1} (Figure 3). This suggests removal of these elements from the solution due to interaction with ZVI and its corrosion products. In contrast, dissolved Mn concentrations increased from <0.02 mgL^{-1} to 4.4 mgL^{-1} and that of Fe even from <0.1 mgL^{-1} to 130 mgL^{-1}. This is related to the dissolution of ZVI granules which have incorporated some Mn as alloying element.

The abrasion product obtained at the end of the experiment had a wet weight of 1.14 kg. According to ICP-MS analyses it contains 28.0 wt% Fe, 17.8 wt% Mo, 7.10 wt% Cr, 4.06 wt% Ca, and 2.36 wt% W (Figure 4). All other elements are below 1 wt%. This fits well to the development of the dissolved concentrations of the respective elements which decreased during the experiments. Considering the mass balance, 160 g Mo were removed from the entire sample of 1000 L, and 203 g Mo were found in the abrasion product. However, considering the water content of the abrasion product, which was not determined, the order of magnitude seems reasonable and clearly demonstrates the capacity of the Ferrodecont process to remove Mo from aqueous solutions. Also for Cr and W concentrations in the abrasion product and the concentration decrease in solution match quite well. After 25 h the Cr concentration increases again which can be interpreted as a rebound effect: Cr which had been adsorbed or precipitated is remobilized by desorption or dissolution [20]. This can be explained by an increase in Eh and O$_2$ concentration in the final stage of the experiment.
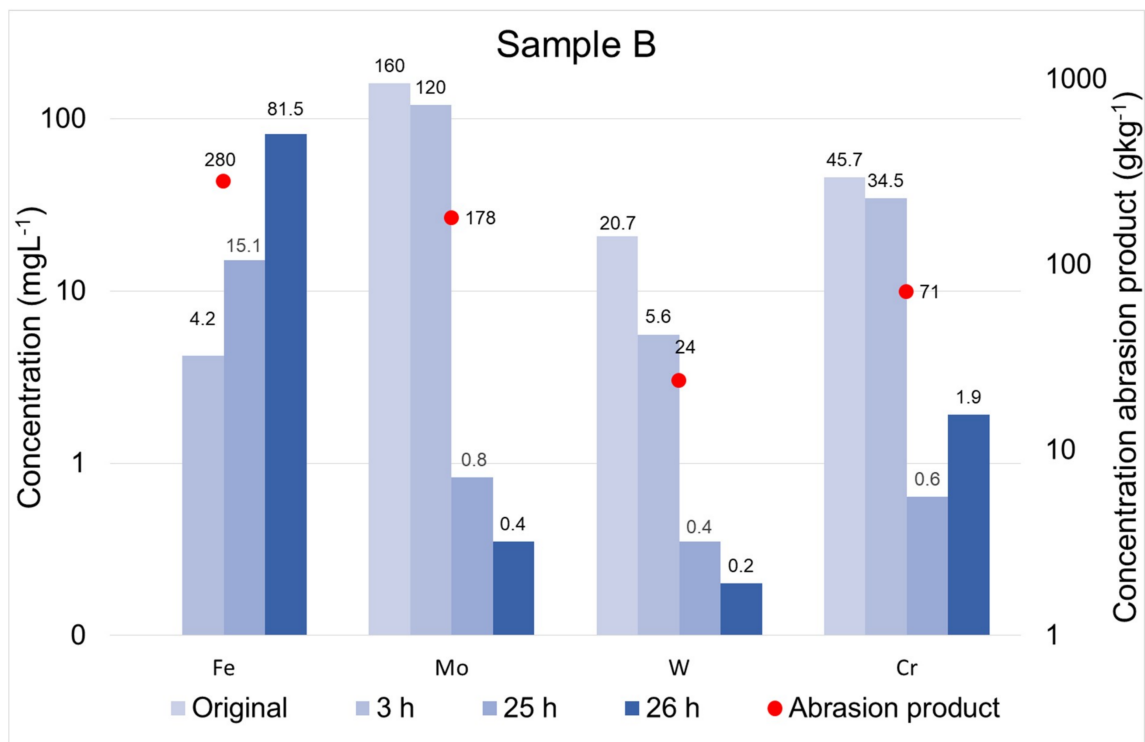
Figure 4. Evolution of the dissolved concentrations (blue bars) and concentrations in the resulting abrasion product (red dots) of Fe, Mo, W, and Cr during the Ferrodecont treatment of sample B.

XRD analyses (Figure 5) of the abrasion product derived from sample B demonstrate that in contrast to the abrasion product obtained from sample A the removed metals do not form distinct crystalline phases. Instead, the XRD pattern shows a very high background, especially in the range between 20 and 45 °2θ which is assigned to amorphous phases. The only crystalline phase is akageneite (ß-FeOOH), a mineral phase which might be considered as a polymorph of goethite but forms at higher Cl concentrations of the aqueous solution and incorporates Cl in its crystal structure [21]. It is suggested that the presence of akageneite and amorphous FeOOH in the abrasion product of sample B is due to higher Cl concentrations and lower pH values (4.0 compared to 4.6 after pH adjustment), respectively, which is in agreement with literature data [22]. Anions were neither determined in the liquid nor in the solid samples, but high alkali metal concentrations in the initial waste water sample B suggest a high salinity. Therefore, it is suggested that akaganeite forms during Ferrodecont treatment of saline waste waters like sample B, whereas goethite and lepidocrocite form during treatment of less saline waste waters. Regarding Mo, Cr and W, two possible mechanisms may occur, the formation of amorphous phases or adsorption onto the surface of akaganeite or amorphous iron phases. As amorphous iron hydroxides are quite abundant whereas amorphous Mo, Cr and W phases are rather exotic, the sorption hypothesis seems more likely and is also supported by a previous study [9]. Comparing the abrasion products of samples A and B, the most striking difference, i.e., the presence of numerous crystalline phases in case of sample A, might not be due to different interactions of the aqueous solutions with ZVI, but rather due to the presence of suspended particulate matter just in sample A, but not in sample B.
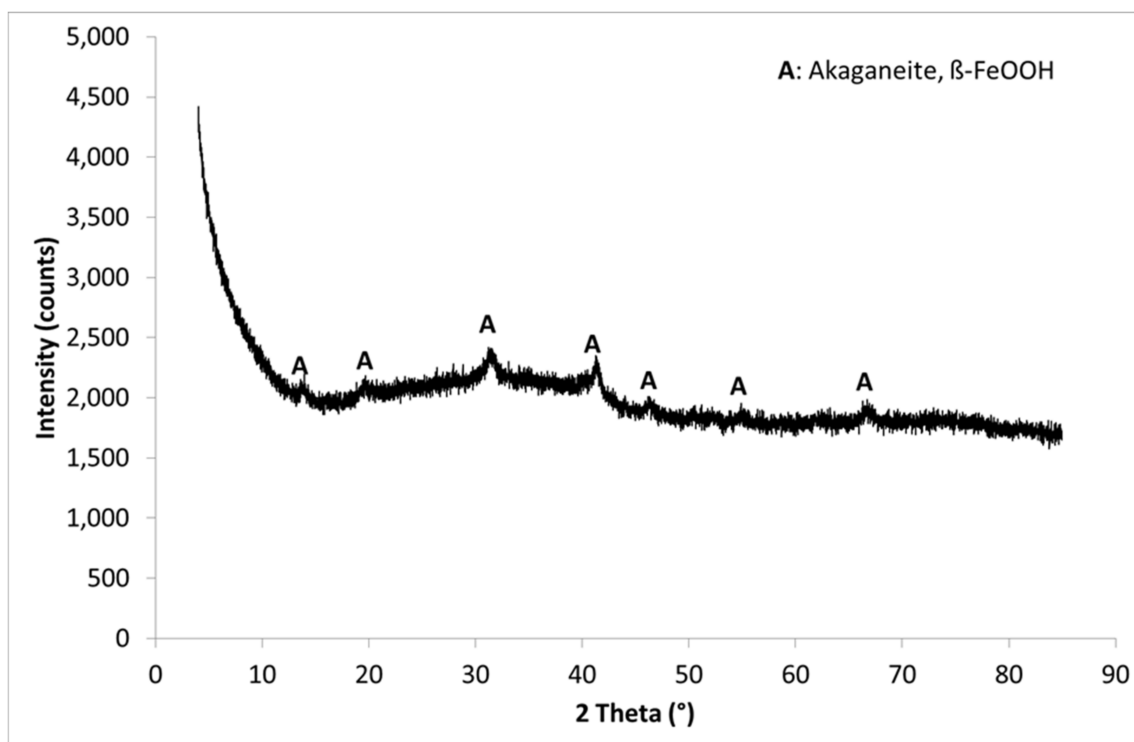
Figure 5. XRD pattern of the abrasion product obtained from Ferrodecont treatment of sample B.

3.4. Thermal Treatment

Thermal treatment of the abrasion product of sample A using STA (Figure 6) shows a slight weight increase (2%) below 100 °C which is associated with a thermal lift. Above 100 °C the weight continuously decreases by more than 25% which is associated with an overall endothermic reaction. At 400 and 500 °C the Gram Schmidt plot, which is the sum of the entire infrared (IR) absorbance of the off-gas flow, shows two distinct peaks. Above 900 °C the weight remains constant, but the endothermic reaction continues. The endothermic peak at about 1075 °C can be related to the melting of copper. Simultaneously, the Gram Schmidt plot indicates again the release of IR-active molecules to the gaseous phase. It has to be mentioned that molecular oxygen, O_2, does not have a dipole momentum and is therefore not IR-active and does not contribute to the Gram Schmidt plot.

The general trend above 100 °C can be explained by the endothermic reduction of Cu(I) to Cu(0) which is associated with the release of O_2. IR measurements (not shown) indicate that the peaks in the Gram Schmidt plot can be assigned to the release of CO_2 and H_2O. It is suggested that FeOOH phases are dehydroxylated which is in agreement with the release of H_2O. However, the source of CO_2 remains unclear, as no carbonates were found in the abrasion products via XRD measurements.

The XRD pattern of the sample that was produced in a vertical furnace at 1300 °C shows an increase in the intensity of the peaks of elemental copper and the neoformation of wuestite (FeO), magnetite (Fe_3O_4), and a hexagonal FeO polymorph (Figure 7) compared to the untreated abrasion product (Figure 2). All mineral phases which contained Cu in its oxidized state in the untreated abrasion product, i.e., delafossite ($CuFeO_2$), cuprite (Cu_2O), paratacamite ($Cu_2(OH)_3Cl$) and calcium copper oxide ($CaCuO_2$), are not detectable anymore.

The reduction of Cu(I) to Cu(0) is in agreement with STA results and with literature data on the Cu–CuO system [23]. Furthermore, Fe(III) was mostly reduced to Fe(II) and only a smaller portion remained present in magnetite (Fe_3O_4). The presence of hexagonal FeO has been described at high pressure [24], but not at low-pressure, high-temperature environments like the experimental setup used for thermal treatment. The observation that Cu can be selectively reduced from the abrasion product is positive with respect to recycling in two ways: Firstly, no further reduction of Cu would be

needed, and secondly, metallic Cu can be more easily separated from the iron phases, either by its higher electric conductivity, different colour, higher density or lower magnetic susceptibility.
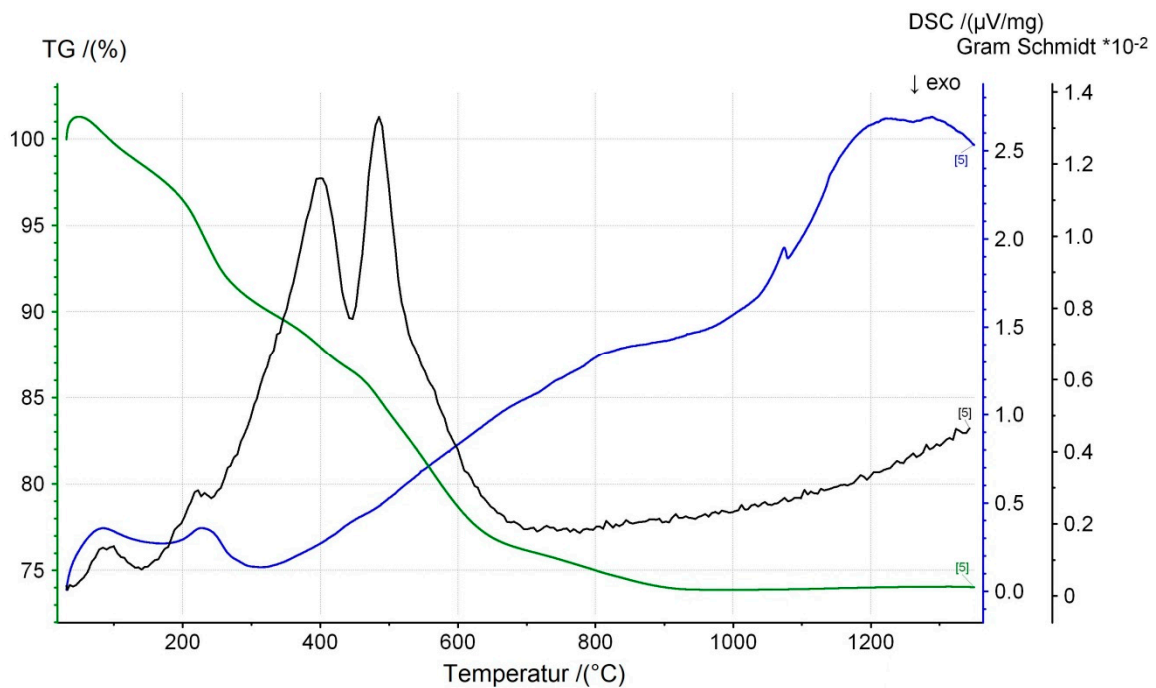

Figure 6. Simultaneous thermal analyses (STA) of the abrasion product of sample A (green line: thermogravimetry (TG), blue line: differential scanning calorimetry (DSC), black line: Gram Schmidt curve).
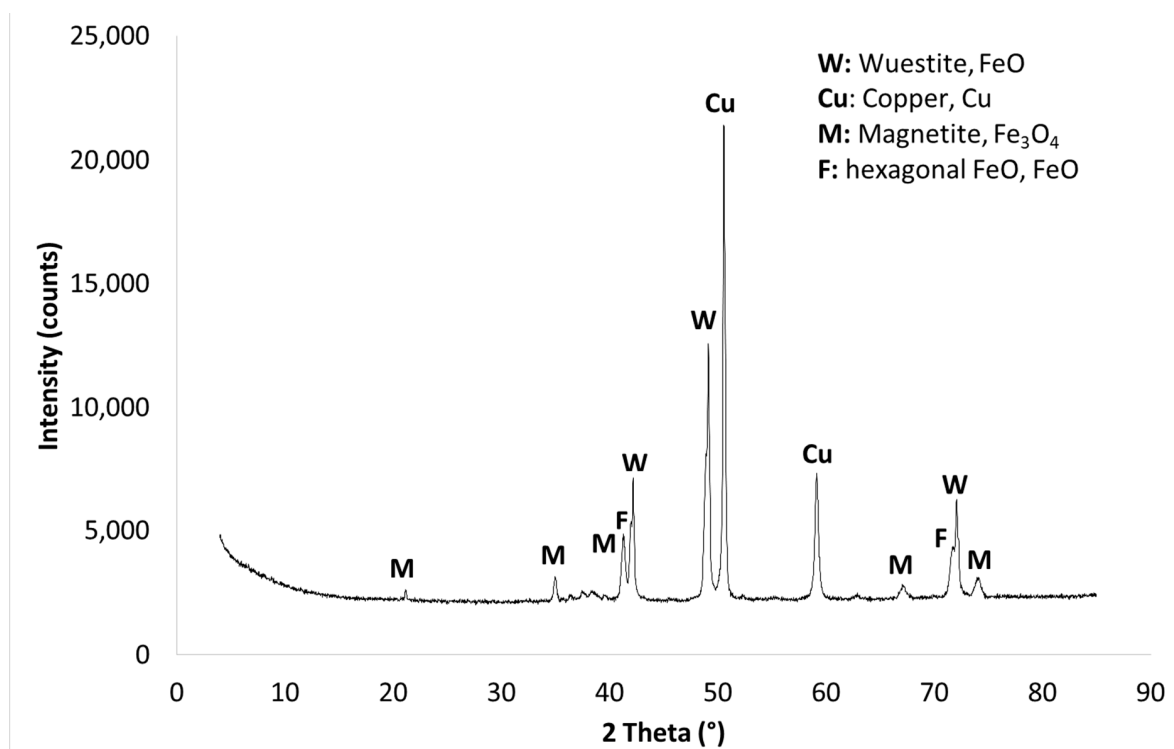

Figure 7. XRD pattern of the thermally treated abrasion product of sample A.

3.5. Magnetic Separation

Magnetic separation of the thermally treated abrasion product using a working distance between magnet and sample of 8 mm yielded a magnetic product which still contains significant amounts of Cu, as Cu particles were intergrown into magnetic iron phases (Figure 8). Decreasing the working distance to 4 mm removed even more iron oxides from the sample, leaving a non-magnetic residue of very high Cu grade. This finding means that simple mineral processing methods can be successfully applied to beneficiate the thermally treated abrasion product and to produce a directly recyclable Cu fraction. However, further attrition (stirring of suspension) or grinding is required for a satisfactory recovery.
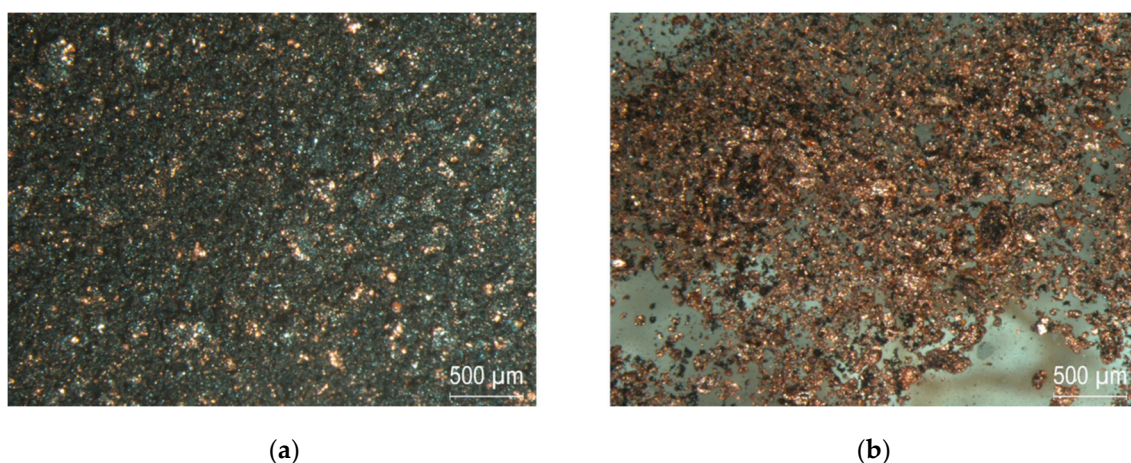

(**a**) (**b**)

Figure 8. Products of magnetic separation of the thermally treated abrasion product of sample A: (**a**) Magnetic product at 8 mm distance between sample and magnet; (**b**) Nonmagnetic residue at 4 mm distance between sample and magnet.

Elemental mappings of the thermally treated abrasion product of sample A support that Cu has been reduced to the elemental state as no oxygen was detected in the Cu-rich area (Figure 9). In summary, these findings demonstrate that in the case of sample A, the residues of the Ferrodecont process can be beneficiated to an easily recyclable Cu concentrate.

3.6. Hydrometallurgical Treatment

Hydrometallurgical treatment (3 d, 1.5 M NaOH, L:S ratio 15:1) of the abrasion product of sample B yielded highly concentrated aqueous extracts, both at 50 and 70 °C. Concentrations of Mo, W, and Cr were in the range of 6 gL^{-1}, 0.8 gL^{-1} and 0.5 gL^{-1}, respectively (Table 2). The concentrations obtained at 50 °C are not lower than those at 70 °C which is economically beneficial as heating is associated with corresponding costs. Contrary, less than 4 mgL^{-1} of Fe were leached which corresponds to an excellent separation between high-value metals and iron. Enrichment of Mo in the extract compared to the concentration in the initial waste water sample B was even 53-fold for the experiment at 50 °C (from 20.7 mgL^{-1} to 6300 mgL^{-1}).

Table 2. Chemical composition of the extracts of hydrometallurgical treatment (3 d, 1.5 M NaOH, L:S ratio 15:1) of the abrasion product of sample B.

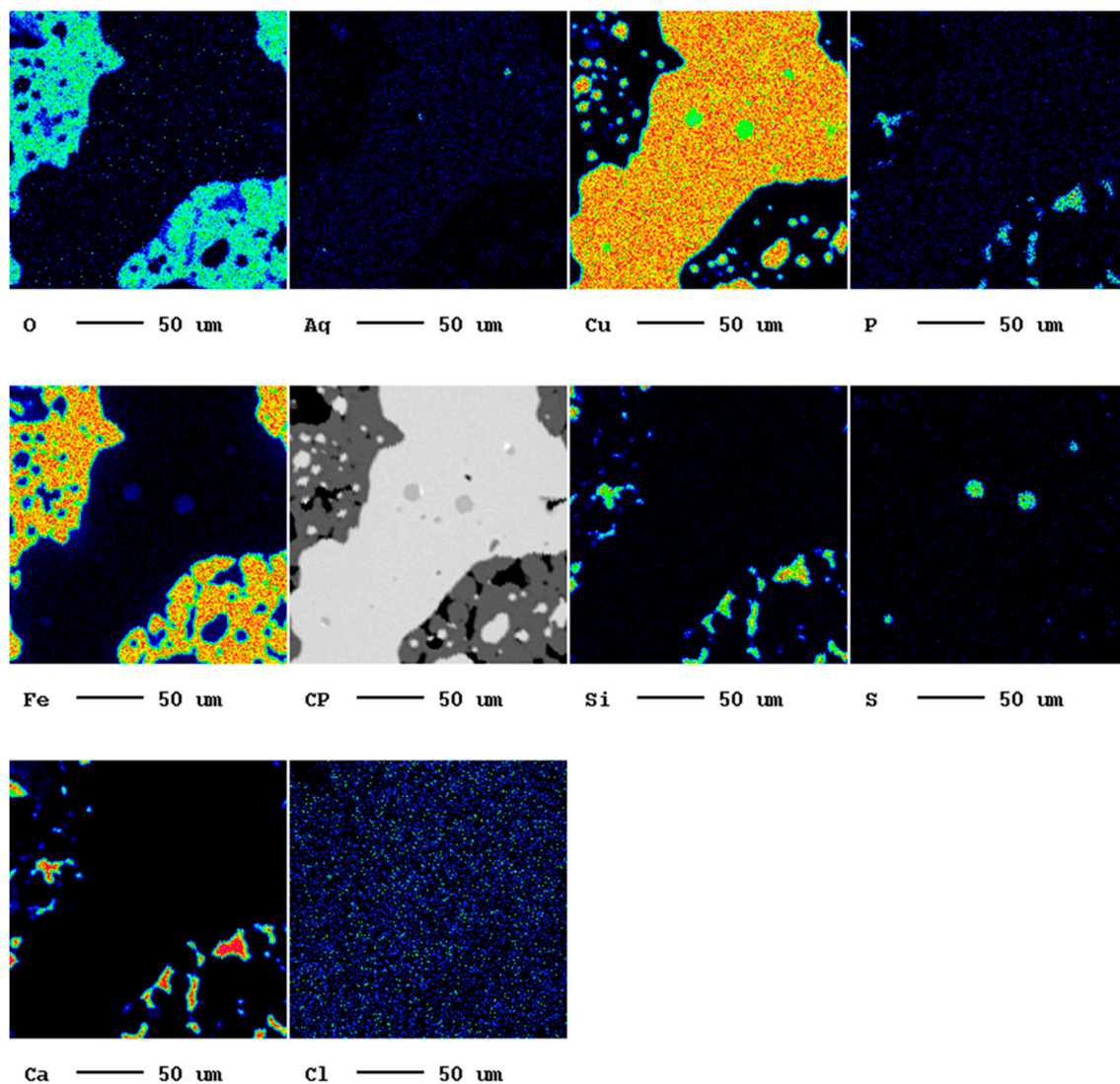| Temperature	Analyte (mgL^{-1})																
	Na	Mg	Si	K	Ca	V	Cr	Mn	Fe	Ni	Cu	Zn	Se	Sr	Mo	Ag	W
50 °C	47200	0.14	510	750	28.6	85.9	460	0.04	3.85	0.18	7.22	0.95	23.7	<0.01	6300	<0.01	840
70 °C	54000	0.09	2220	660	10.9	87.2	460	0.02	2.94	0.41	1.61	0.18	17.2	<0.01	5820	<0.01	800

Figure 9. Elemental mappings of the same observed area the thermally treated abrasion product of sample A.

The observed behaviour can be explained by the occurrence of Mo, W, and Cr as oxyanions, i.e., molybdate (MoO_4^{2-}), tungstate (WO_4^{2-}), and chromate (CrO_4^{2-}) [25]. At alkaline pH the surface of the mineral phases in the abrasion product consists of, i.e., iron oxyhydroxides, are negatively charged due to the high dissolved concentration of OH^- ions. These ions hydroxylate the dangling bonds at the crystal surface which creates a negative charge of the mineral surface. Consequently, the adsorbed oxyanions are desorbed from the surface due to the repelling effect of equal charges, and released into the solution.

Remaining solids mainly contained Fe (31.7 and 27.1 wt% for 50 and 70 °C) and only little concentrations of Cr (5.62 and 5.55 wt%), Mo (2.01 and 1.68 wt%), and W (0.34 and 0.25 wt%). Furthermore, significant amounts of Na (5.19 and 4.31 wt%), Si (0.64 and 2.15 wt%), and Ca (1.78 and 1.79 wt%) were detected, whereas the concentrations of all other elements were below 1 wt%. The chemical composition of the residues might allow a valorisation in the iron and steel industry.

4. Conclusions

In this study we integrated a granular bed reactor using ZVI, the so-called Ferrodecont process, into an entire value chain by further treatment of the obtained abrasion products using tailored technologies,

i.e., a combination of thermal treatment and magnetic separation for Cu-containing abrasion products and a hydrometallurgical treatment for abrasion products containing oxyanions. In both cases, directly recyclable intermediate products containing up to 53 times the initial concentrations of valuable elements were obtained. For further application it is necessary to scale-up and optimise the solid:liquid separation and the thermal treatment. The existing weakness of our approach is that for every waste water a different beneficiation route has to be found. A possible solution might be a modular machine which can be adapted to waste waters by replacing the beneficiation units depending on the requirements. Material flow monitoring in the beginning of the process, e.g., by sensor technology, combined with machine learning may be used to control the entire process chain and automatically select the appropriate process route.

Author Contributions: Conceptualization, D.V., P.M., R.M. and K.P.S.; methodology, D.V., P.M., R.M., F.K., W.Ö., K.P.S.; investigation, K.P., P.M., R.M., F.K., W.Ö. and K.P.S.; resources, P.M., R.M., F.K., W.Ö., K.P.S.; writing—original draft preparation, D.V., K.P.S.; writing—review and editing, D.V., S.N., P.M., R.M.; F.K., W.Ö., K.P.S.; visualization, K.P.S., S.N.; supervision, D.V., K.P.S.; project administration, K.P.S.; funding acquisition, D.V. All authors have read and agreed to the published version of the manuscript."

Conflicts of Interest: The authors declare no conflict of interest. The funders had no role in the design of the study; in the collection, analyses, or interpretation of data; in the writing of the manuscript, or in the decision to publish the results.

References

1. European Commission. Communication from the Commission to the European Parliament, the Council, the European Economic and Social Committee and the Committee of the Regions on the 2017 list of Critical Raw Materials for the EU. Document 52017DC0490. 2017. Available online: https://eur-lex.europa.eu/legal-content/EN/TXT/?uri=CELEX%3A52017DC0490 (accessed on 26 February 2020).

2. Vollprecht, D.; Krois, L.-M.; Sedlazeck, K.-P.; Müller, P.; Mischitz, R.; Olbrich, T.; Pomberger, R. Removal of critical metals from waste water by zero-valent iron. *J. Clean. Prod.* **2019**, *208*, 1409–1420. [CrossRef]

3. Austrian Federal Minister for Agriculture and Forestry. General Waste Water Emission Ordinance. 1996. Available online: https://www.ris.bka.gv.at/GeltendeFassung.wxe?Abfrage=Bundesnormen&Gesetzesnummer=10010977 (accessed on 26 February 2020).

4. Wagner, M.; Menapace, H.; Frate, R. Stand der Technik bei der Chemisch-Physikalischen Behandlung von Flüssigen Abfällen. 2010. Available online: http://www.abfallwirtschaft.steiermark.at/cms/dokumente/11270827_135033048/b1aa5b46/Endversion%20SdT-Studie%20CP-Anlagen%2020100130%20Deckblatt_.pdf (accessed on 21 October 2019).

5. Müller, P.; Lorber, K.E.; Mischitz, R.; Weiss, C. Implementation of fluidized granulated iron reactors in a chromate remediation process. *Sci. Total Environ.* **2014**, *485*, 748–754. [CrossRef]

6. Noubactep, C. Metallic iron for environmental remediation: A review of reviews. *Water Res.* **2015**, *85*, 114–123. [CrossRef] [PubMed]

7. Sedlazeck, K.P.; Vollprecht, D.; Müller, P.; Mischitz, R.; Gill, J.; Trois, W.; Maunz, I.; Frate, R.; Mann, O.; Wruss, K. Decomposition of dissolved organic contaminants bycombining a boron-doped diamond electrode, zero-valent iron and ultraviolet radiation. *Chemosphere* **2019**, *217*, 897–904. [CrossRef] [PubMed]

8. Moon, E.; Peacock, C. Adsorption of Cu(II) to ferrihydrite and ferrihydrite–bacteria composites: Importance of the carboxyl group for Cu mobility in natural environments. *Geochim. Cosmochim. Acta* **2012**, *92*, 203–219. [CrossRef]

9. Gustafsson, J.P. Modelling molybdate and tungstate adsorption to ferrihydrite. *Chem. Geol.* **2003**, *200*, 105–115. [CrossRef]

10. Afkhami, A.; Norooz-Asl, R. Removal, preconcentration and determination of Mo(VI) from water and wastewater samples using maghemite nanoparticles. *Colloids Surf. A* **2009**, *346*, 52–57. [CrossRef]

11. Kashiwabara, T.; Takahashi, Y.; Marcus, M.; Uruga, T.; Tandia, H.; Terada, Y.; Usui, A. Tungsten species in natural ferromanganese oxides related to its different behaviour from molybdenum in oxic ocean. *Geochim. Cosmochim. Acta* **2013**, *106*, 364–378. [CrossRef]

12. Kishimoto, N.; Iwano, S.; Narazaki, Y. Mechanistic Consideration of Zinc Ion Removal by Zero-Valent Iron. *Water Air Soil Pollut.* **2011**, *221*, 183–189. [CrossRef]

13. Wang, S.; Zhao, M.; Zhao, Y.; Wang, N.; Bai, J.; Feng, K.; Zhou, Y.; Chen, W.; Wen, F.; Wang, S.; et al. Pyrogenic temperature affects the particle size of biochar-supported nanoscaled zero valent iron (nZVI) and its silver removal capacity. *Chem. Spec. Bioavailab.* **2017**, *29*, 179–185. [CrossRef]

14. Perales-Perez, O.; Umetsu, Y. Ambient-temperature precipitation of Zn ions from aqueous solutions as ferrite-type compounds. *Hydrometallurgy* **2002**, *63*, 235–248. [CrossRef]

15. Austrian Standards 2017, ÖNORM EN ISO 17294-2. Water quality—Application of Inductively Coupled Plasma Mass Spectrometry (ICP-MS) Part 2: Determination of Selected Elements Including Uranium Isotopes. Available online: https://www.iso.org/standard/62962.html (accessed on 28 February 2020).

16. Austrian Standards 2002, ÖNORM EN 13657. Characterization of Waste—Digestion for Subsequent Determination of Aqua Regia Soluble Portion of Elements. Available online: https://infostore.saiglobal.com/en-us/Standards/PN-EN-13657-2006-930012_SAIG_PKN_PKN_2193021/ (accessed on 28 February 2020).

17. Heinemann, M.; Eifert, B.; Heiliger, C. Band structure and phase stability of the copper oxides Cu_2O, CuO, and Cu_4O_3. *Phys. Rev. B* **2013**, *87*, 11511. [CrossRef]

18. Pfandl, K.; Küppers, B.; Scheiber, S.; Stockinger, G.; Holzer, J.; Pomberger, R.; Antrekowitsch, H.; Vollprecht, D. X-ray fluorescence sorting of non-ferrous metal fractions from municipal solid waste incineration bottom ash processing depending on particle surface properties. *Waste Manag. Res.* **2020**, *38*, 111–121. [CrossRef]

19. Cui, J.; Zhang, L. Metallurgical recovery of metals from electronic waste: A review. *J. Hazard. Mater.* **2008**, *158*, 228–256. [CrossRef]

20. Sedlazeck, K.P.; Vollprecht, D.; Müller, P.; Mischitz, R.; Gieré, R. Impact of an in-situ Cr(VI)-contaminated site remediation on the groundwater. *Environ. Sci. Pollut. Res.* **2020**. [CrossRef]

21. Morcillo, M.; González-Calbet, J.M.; Jiménez, J.A.; Díaz, I.; Alcántara, J.; Chico, B.; Mazarío-Fernández, A.; Gómez-Herrero, A.; Llorente, I.; de la Fuente, D. Environmental Conditions for Akaganeite Formation in Marine Atmosphere Mild Steel Corrosion Products and Its Characterization. *Corrosion* **2015**, *71*, 872–886. [CrossRef]

22. Misawa, T.; Hashimoto, K.; Shimodaira, S. The Mechanism of Formation of Iron Oxide and Oxyhydroxides in Aqueous Solutions at Room Temperature. *Corros. Sci.* **1974**, *14*, 131–149. [CrossRef]

23. Rakhshani, A.E. Preparation, Characteristics and Photovoltaic Properties of Cuprous Oxide—A Review. *Solid-State Electron.* **1986**, *29*, 7–17. [CrossRef]

24. Mazin, I.; Fei, Y.; Downs, R.; Cohen, R. Possible polytypism in FeO at high pressures. *Am. Mineral.* **1998**, *83*, 451–457. [CrossRef]

25. Takeno, N. Atlas of Eh-pH Diagrams. Intercomparison of Thermodynamic. Geological Survey of Japan Open File Report No. 419. 2005. Available online: http://www.eosremediation.com/download/Chemistry/Chemical%20Properties/Eh_pH_Diagrams.pdf (accessed on 18 February 2020).